

# REALIZATION OF INVAR ALLOY LNG PIPING

Takehiko Edamitsu; Osaka Gas Co., Ltd.

Shuji Yamamoto; Osaka Gas Co., Ltd.

Muneji Ujita; Osaka Gas Co., Ltd.

Takeo Yamakawa; Kawasaki Heavy Industries, Ltd.

Setsuji Kishimoto; Kawasaki Heavy Industries, Ltd.

Keiichi Nakamura; Sumitomo Metal Industries, LTD.

Keiichi Yamamoto; Sumitomo Metal Industries. LTD.

## 1. INTRODUCTION

Osaka Gas Co., Ltd., Kawasaki Heavy Industries, Ltd. and Sumitomo Metal Industries, LTD. developed Invar alloy LNG piping for the purpose of reduction of LNG piping construction costs, and the practical application of an Invar alloy LNG piping was achieved in 2001 for the first time in the world. Following this first application of Invar alloy LNG piping that serves as an interconnection piping to an LNG vaporizer, Invar alloy LNG piping including large diameter one as an interconnection piping to an LNG tank is under construction and will be commissioned in August, 2003.

This report summarizes the contents of research, development and realization of Invar alloy LNG piping.

## 2. PURPOSE OF DEVELOPMENT OF INVAR ALLOY LNG PIPING

Osaka Gas has LNG receiving terminals at Senboku (Terminals I and II) and Himeji where a total of several tens of kilometers of LNG piping is installed for receiving and discharging LNG as well as for interconnecting various facilities. Since LNG is cryogenic fluid of 111K, austenitic stainless steel is used for LNG piping.

Austenitic stainless steel has excellent low-temperature characteristics and stable quality. However, due to its large coefficient of linear expansion, austenitic stainless steel requires a mechanism for absorbing thermal contraction up to approximately 3 mm per meter when it is used in LNG facilities. The mechanism that Osaka Gas generally uses for its LNG piping is a bent piping (Photo. 1).

A bent piping, which is installed every 30 to 70 m, raises the cost of LNG piping construction as outlined below.

- (1) The cost of pipe material increases due to increase in the number of additional elements to form a bend, e.g. bent pipes and short straight pipes.
- (2) The cost of welding work and welding inspections increases due to increase in the number of welded joints.
- (3) The cost of cold insulation increases due to increase in additional insulation work for bends, which is especially labor-intensive.
- (4) The diameter of pipe may have to be enlarged in order to compensate increased pressure loss caused by a larger number of bends.
- (5) Since bent piping requires a large amount of space, when LNG piping is installed in a tunnel for example, the diameter of a tunnel may have to be enlarged in order to accommodate it.



Photo. 1 Austenitic Stainless Steel Bent Piping for LNG service

Because Invar alloy has coefficient of linear expansion, which is, approximately 1/10 that of austenitic stainless steel, the Invar alloy piping eliminates the need for bend piping. Despite the higher cost of Invar alloy material itself, the total construction cost can be reduced as a result of straight piping without bent piping and the elimination of the abovementioned cost raising factors.

The purpose of the present development is to apply Invar alloy for LNG piping. This development will lead to reducing the cost of LNG piping significantly, based on simple piping structures with only straight lines. For example, in the case of a large receiving piping of LNG terminal in Japan, application of Invar alloy can reduce the cost by approximately 20%.

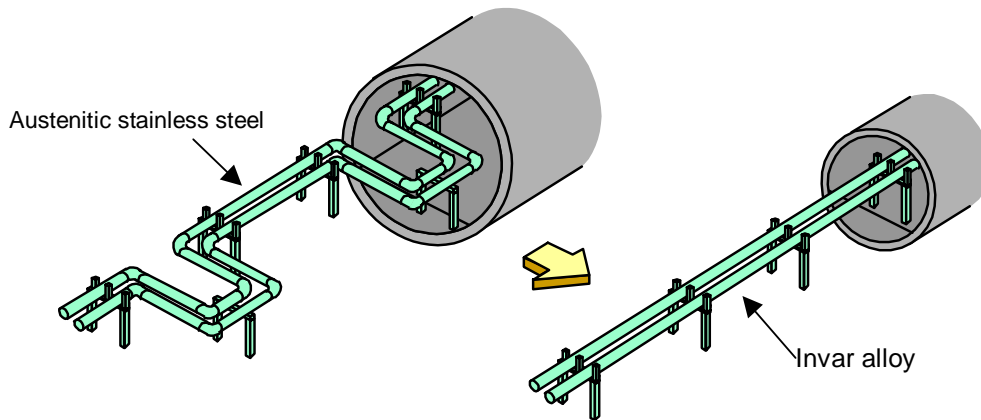


Fig.1 Conceptual view of Invar alloy LNG piping

### 3. FEATURES OF INVAR ALLOY

#### 3.1 Material characteristics

Invar alloy, an alloy of 64% Fe-36% Ni, has a very low coefficient of linear expansion. Fig 2 shows correlation between Ni content of Fe-Ni alloy and its coefficient of linear expansion. The coefficient of linear expansion reaches the minimum value at 36% Ni content. Table 1 shows standard, characteristic values of Invar alloy. Since Invar alloy has a stable austenitic structure, it has excellent strength and ductility at LNG temperature.

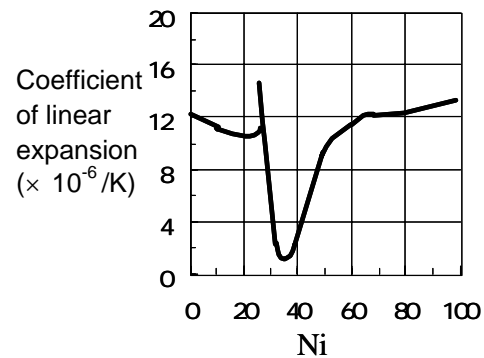


Fig. 2 Ni% in Fe-Ni alloy and coefficient of linear expansion MOL(vol.90.9)

Table 1 Strength characteristics

Item	Invar alloy	Austenitic stainless steel
0.2% proof stress	> 240 N/mm <sup>2</sup>	> 205 N/mm <sup>2</sup>
Tensile strength	> 440 N/mm <sup>2</sup>	> 520 N/mm <sup>2</sup>
Elongation	> 30 %	> 40 %

#### 3.2 Previous Applications of Invar Alloy

Invar alloy has been used as a functional material in special applications in which low thermal expansion is essential, such as CRT shadow masks and tension members (core material) of overhead power transmission lines, but it has seldom been used as a thick-walled structural material. As for LNG applications, Invar alloy is widely used as membranes for LNG carrier cargo tanks, but their thickness is limited to 0.7 to 1.7 mm.

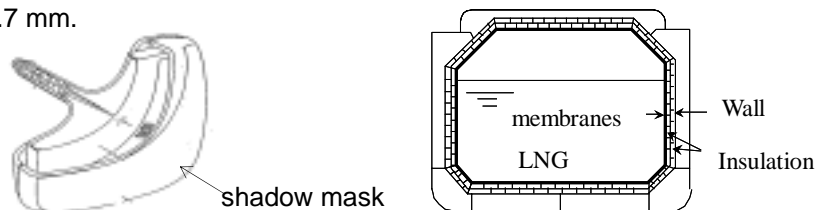


Fig. 3 Examples of Invar alloy applications: CRT and LNG carrier

## 4. OUTLINE OF DEVELOPMENT OF INVAR ALLOY LNG PIPING

In our research and development, efforts were focused on the examination, experimentation and evaluation of Invar alloy's material characteristics, weldability, design, nondestructive inspection and corrosive resistance. These activities led to the establishment of technology and the practical application of Invar alloy LNG piping.

### 4.1 Investigation of Invar Alloy's Material Characteristics

The characteristics of Invar alloy are described in various technical documents and manufacturers' catalogues, but those data are often fragmentary or insufficient to allow proper designing of pressure parts. Therefore, the tests were conducted in a temperature range from ambient to cryogenic in order to obtain data of the material characteristics of Invar alloy including its welds, such as physical properties, strength and toughness. Then, based on these test results, the standard values of characteristics necessary for designing Invar alloy LNG piping were established.

Fig.4 shows measurements of tensile strength and 0.2% proof stress of Invar alloy, as an example.

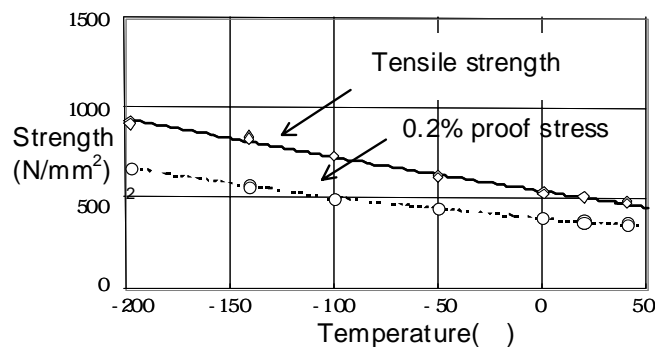


Fig. 4 Invar alloy strength characteristics

Moreover, design fatigue curves of Invar alloy were established on the basis of measurements.

### 4.2 Establishment of Welding Technology

Welding of Invar alloy had a problem of ductility-dip cracks in weld metal in the case of multi-pass welding process. In this research, the mechanism of ductility-dip cracks of Invar alloy was clarified, and filler wires for GTAW were developed which have excellent ductility and prevent ductility-dip cracks. Then appropriate welding procedures (welding process, heat input, etc.) using the developed welding materials were established.

#### 4.2.1 The Weld Cracking Mechanism

To investigate the mechanism of crack generation in the multi-pass welding of Invar alloy, macrostructural observation (Photo.2), microstructural observation, and a high-temperature ductility test were conducted.

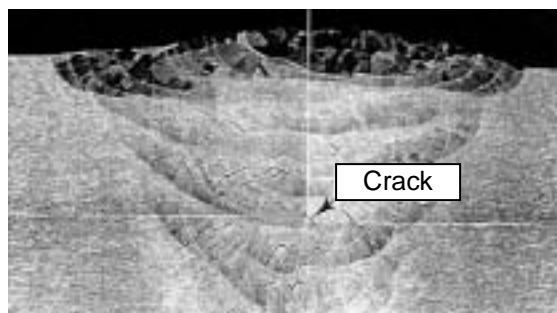


Photo.2 Ductility dip cracks in multi-pass GTAW weld metal of Invar alloy

The results of these studies were analyzed in terms of location of crack, temperature rise caused by subsequent weld passes, and temperature ranges where ductility of weld metal degrades. These metallurgical investigations identified cracks observed in multi-pass welds of Invar alloy as ductility dip cracks, which occurred as a result of the ductility of the weld metal being degraded due to reheating by subsequent weld passes.

Furthermore, to study the influence of the sulfur (S) content in the weld metal on susceptibility to ductility dip cracks of Invar alloy, a double-bead longitudinal Varestraint test was carried out. Based on the results, it was confirmed that susceptibility of Invar alloy to ductility dip cracks grew higher as the amount of S increased. Auger electron spectroscopy conducted on a fracture surface obtained by rupturing the weld metal in an ultra-high vacuum revealed a peak of S only at the grain boundary to indicate its segregation.

Based on these findings, it was concluded that ductility dip cracks in the multi-pass welding of Invar alloy were caused by segregation of S that reduced the bonding strength at the grain boundary.

#### 4.2.2 Prevention of weld defects

In order to establish a method to prevent ductility dip cracks that occur in Invar alloy during the multi-pass welding process, the effect of the chemical composition of the weld metal and its mechanism were examined. Investigation of various additional elements for the filler wire for GTAW determined that complex addition of carbon (C) and niobium (Nb) was effective for preventing ductility dip cracks.

Fig. 5 shows the effect of C and Nb on the total length of ductility dip cracks generated in the bead during a double-bead longitudinal Varestraint test.

Ductility dip cracks occurrence was confirmed to decrease as the amounts of C and Nb were increased. When these elements were added individually, cracks were generated in the weld metal, but the complex addition of the two elements prevented cracks.

Photo 3 shows microstructures of two types of weld metal; one with C and Nb added, and another without. The solidified 0.01%C-0%Nb morphology with ductility dip cracks revealed a straight grain boundary (cellular structure), while the 0.2%C-0.8%Nb morphology without ductility dip cracks indicated a zigzag cellular boundary (cellular dendrite crystal).

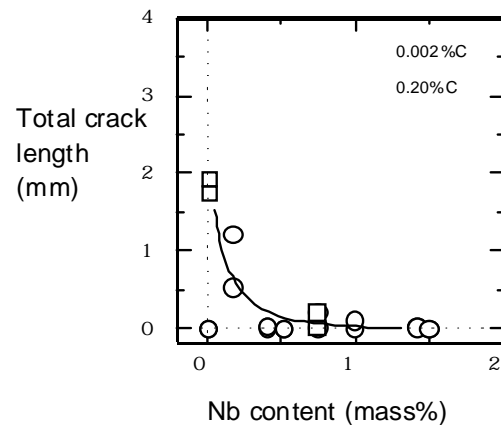


Fig. 5 Effect of C, Nb content on ductility dip crack prevention

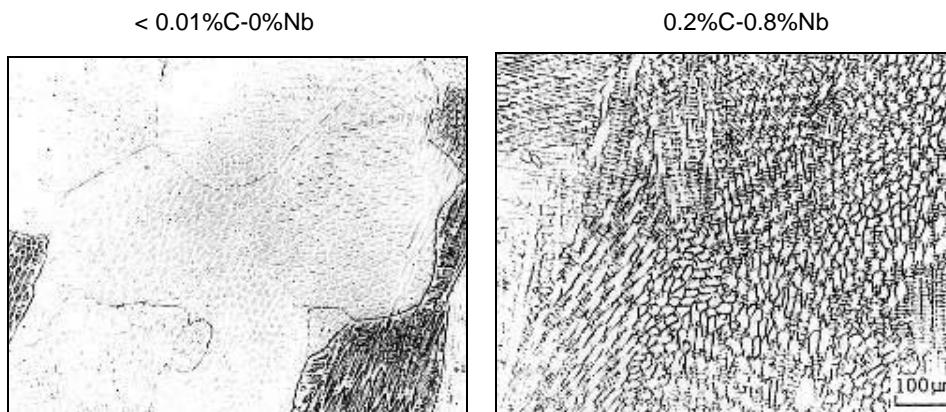


Photo. 3 Microstructure of Invar alloy weld metal

This observation, combined with the identification of the grain boundary deposit, led to the

conclusion that Invar alloy's susceptibility to ductility dip cracks was suppressed by the combined addition of C and Nb because the two elements resulted in the crystallization of niobium carbide (NbC) at the grain boundary, making the grain boundary structure complex and increasing its area to reduce segregation of S and the stress concentration at the grain boundary triple point.

#### 4.2.3 Establishment of Welding Method

The results of investigation determined that the addition of C and Nb to the filler wire for GTAW could prevent ductility dip cracks in Invar alloy. However, an excessive amount of C and Nb can lower the ductility of the weld. Therefore, experiments were conducted using two types (low Nb and high Nb; refer to Table 2) of filler wires to determine welding conditions quantitatively that would ensure the prevention of ductility dip cracks and also secure the required ductility for use of Invar alloy in low-temperature LNG conditions.

Table 2 Chemical compositions of materials used (mass.%)

Material		C	Si	Mn	P	S	Ni	Nb
Base metal (9.5mm <sup>t</sup> )		0.003	0.03	0.19	0.005	0.001	35.99	
Filler wire (1.2mm)	H 1	0.23	0.03	0.20	0.001	<0.001	36.44	0.80
	H 2	0.22	<0.01	0.12	0.001	<0.001	35.98	1.61

Multi-pass GTAW was conducted on Invar alloy plates measuring 9.5 mm x 200 mm x 100 mm and having a U-shape groove (see Fig. 6). In this welding test, constant welding conditions were maintained for the first and the second deposition layers indicated by the shaded area in the diagram, and heat input and wire feeding rate for the third and the subsequent layers were varied.

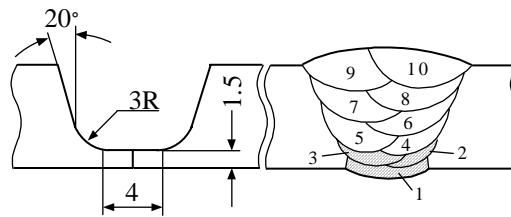


Fig. 6 Groove geometry and deposition sequence used

Fig. 7 shows the relationship between crack occurrence and weld conditions, i.e., heat input and wire feeding rate for the third and the subsequent deposition layers in all-layer welding using the low-Nb filler wire (H1). There were no ductility dip cracks at the points indicated with the white dots in the graph, and ductility dip cracks were observed at the points indicated with the black dots. The graph shows that ductility dip cracks occurred when heat input was high and wire feeding rate was low. The cracks were observed in the first half of the layers. It was presumed that these cracks were generated because the dilution rate of C and Nb added to prevent ductility dip cracks was higher at the bottom of the U-shaped groove.

To verify this, welding tests were performed using the high-Nb filler wire (H2) for the first and the second deposition layers, and the low-Nb wire (H1) for the third and the subsequent layers. Fig. 8 shows the relationship between the heat input/wire feeding rate and the presence of ductility dip cracks. As shown in the diagram, the abovementioned welding technique prevented the generation of ductility dip cracks under entire test conditions. In the diagram, the figures in circles indicate Charpy impact values at the test temperature of 77K, and the figures above the circles indicate the average Nb content of the weld metal.

As stated above, the combined addition of C and Nb in the filler wire prevented ductility dip cracks and also achieved welds with sufficient ductility under low temperatures. Based on these results, standard Invar alloy welding procedures were established for two cases: welding of Invar alloy

pipes and pipe joints during manufacture, and welding conducted at installation sites.

A standard welding procedure was also established for preventing ductility dip cracks and securing low temperature ductility of weld of dissimilar materials -- Invar alloy and austenitic stainless steel -- that will be required in LNG facilities.

Moreover, standard procedures for fillet welding and repair welding were established. All the established standard welding procedures are applicable to automatic GTAW, manual GTAW, and the combination of them.

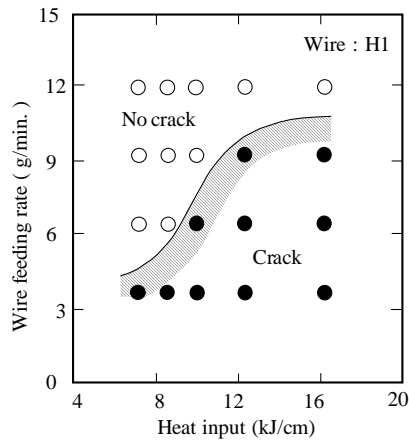


Fig.7 Relationship between ductility dip crack occurrence and welding conditions

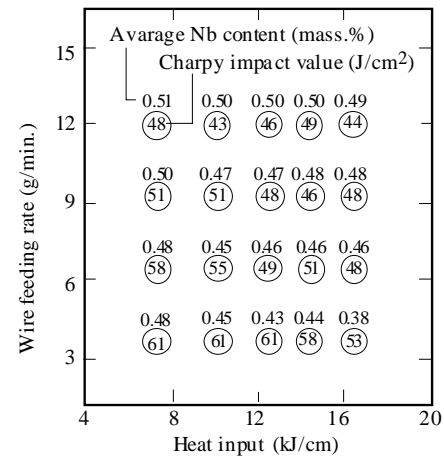


Fig.8 Nb content and Charpy impact value of weld metal under various heat input and wire feeding rate (the third pass and after)

#### 4.2.4 Evaluation of Safety of Weld

The materials of LNG piping including their welds are required to have sufficient ductility to inhibit unstable fracture under a low temperature of 111K. Because Invar alloy is an austenitic alloy, it is not susceptible to brittle fracture. Therefore, a ductile fracture resistance test was conducted to evaluate Invar alloy's susceptibility to ductile unstable fracture and ductile cracks initiation. The test results verified a high level of safety against fracture of Invar alloy LNG piping joints welded in accordance with the standard welding procedures established in this development. The critical crack dimension obtained during the test was confirmed to be within the detectable range by comparing them with the flaw detection performance of a radiographic testing (RT).

### 4.3 Design

#### 4.3.1 Design method

Various design factors of Invar alloy piping were organized including types and combinations of loads applied to LNG piping, calculation methods and allowable stress, and trial design of a model case was performed. This model case verified that the generated stress was below the allowable value even without bent piping.

#### 4.3.2 Piping support structure

The support structure for Invar alloy LNG piping is required to have the following performance..  
High insulation performance

Bearing performance for high longitudinal load due to eliminating the bent piping

Fig. 8 shows an example of the established support structure

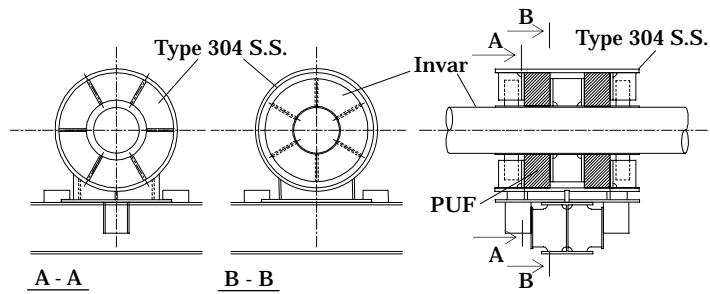


Fig.9 Example of axial stop for Invar alloy LNG piping

#### 4.3.2 Evaluation of Weld of Dissimilar Materials

FEM analysis and thermal stress measurement using an actual joint were conducted to investigate the thermal stress behavior around welds of dissimilar materials, i.e., Invar alloy and austenitic stainless steel, under low temperatures. The analysis and measurement results indicated that the generated thermal stress intensity was within the allowable value, and confirmed that the weld was robust even after repeated cooling and heating in a pressurized condition. Furthermore, a method was established for the theoretical analysis of the thermal stress behavior of welds of dissimilar materials.

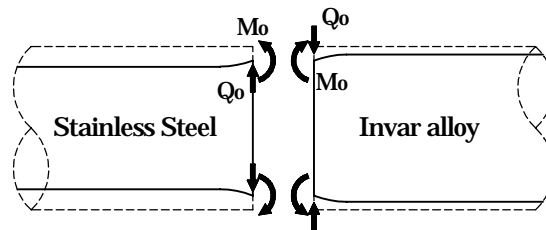


Fig.10 Deformation and constraint forces at dissimilar joint boundary

#### 4.3.4 Insulation structure

An insulation structure was established for preventing decline in insulation performance caused by expansion of the gap between each block of polyurethane foam in low temperature condition caused by difference of coefficient of linear expansion between Invar alloy and polyurethane foam. Fig.9 shows the structure of insulation.

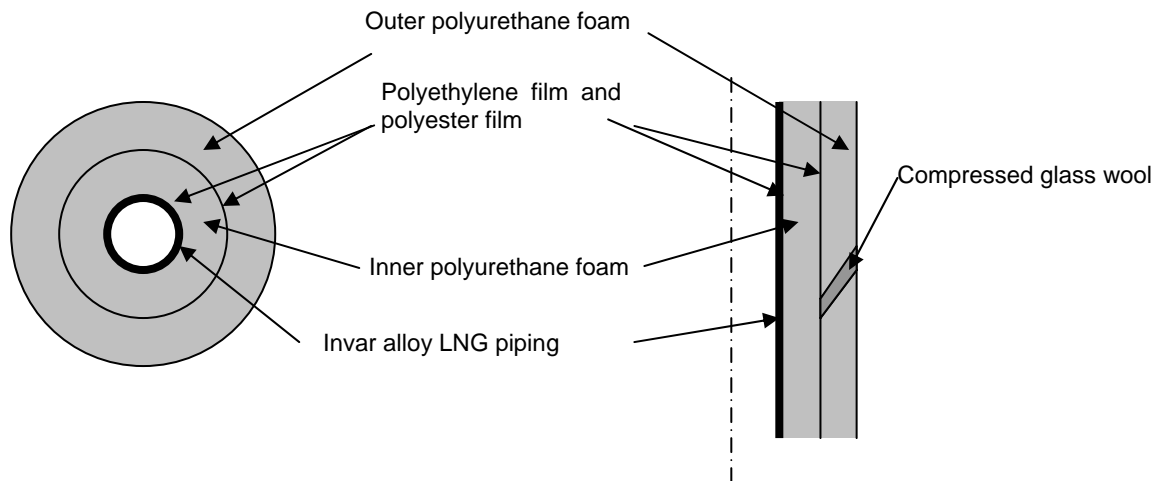


Fig. 11 Insulation structure for preventing expansion of the gap

Between invar alloy LNG piping and insulation, and between inner insulation and outer insulation, polyethylene films are installed for sliding. Compressed glass wool is stuffed in the gap between the polyurethane blocks. It expands when the gap extends due to thermal contraction of polyurethane blocks. The gap is slanted to elongate the pass of thermal conduction.

This structure was tested under the low temperature of LNG, and its performance was confirmed.

#### 4.4 Inspection (Establishment of Nondestructive Inspection Method)

For nondestructive inspections of LNG piping welds of austenitic stainless steel (Type 304), a penetration testing (PT) is usually conducted for surface flaw detection, and a radiographic testing (RT) for internal defects. The same inspection methods would be used for Invar piping welds.

Although the difference of materials does not cause any difference in the surface flaw detection accuracy of the PT, it can result in a fluctuation of the internal flaw detection accuracy of the RT. When conducting the RT on Invar alloy with a high Ni content, its large attenuation of radiation has to be taken into consideration.

RT was carried out for Invar alloy with artificial flaws under various conditions in accordance with JIS Z 3106-1971 "Methods of radiographic test and classification of radiographs for stainless steel welds", and a standard RT method for Invar alloy was established which provides the same flaw detection accuracy as for Type 304 stainless steel.

#### 4.5 Stress Corrosion Cracking (SCC) and the Establishment of SCC Prevention Method

Corrosive characteristics of Invar alloy were tested, and the results of this research indicated that Invar alloy was more susceptible to SCC than stainless steel when residual stress from welding was present. Therefore, Invar alloy's susceptibility to SCC was investigated in detail, and its prevention method was established.

##### 4.5.1 Invar Alloy's Susceptibility to SCC

Invar alloy's characteristics on SCC were studied using the 4-point bend-beam method (ASTM G39-73) in a simulated marine atmosphere. Susceptibility to SCC was evaluated based on the maximum depths of cracks in the cross sections of specimens measured by microstructural observation. Table 3 shows the results of the measurement.

Table 3 Results of SCC test of Invar alloy in the simulated marine atmosphere with adhered airborne salt for 1000h

Temp (K)	RH (%)	Invar alloy				304S.S.	
		Amount of adhered airborne salt (g/m <sup>2</sup> )					
		0.02	0.2	2.0	20.0		
313	80				x		
333	60	x	x	x	x		
	80	x	x	x	x	x	

: No SCC

: SCC(Maximum depth of crack is less than 100 μm)

x : SCC(Maximum depth of crack is more than 100 μm)

The test results indicated that Invar alloy was susceptible to SCC in an atmosphere with adhered airborne salt and the depths of cracks were larger when the temperature was higher. The generated SCC was of a transgranular type (TG-SCC) initiated from pitting.

##### 4.5.2 SCC Prevention Method

To prevent SCC of Invar alloy, examinations were performed for a method of applying residual surface compressive stress with sandblasting and the use of zinc-rich painting. The test results showed that sandblasting treatment was effective for the prevention of SCC. This method is expected to be more effective when combined with zinc-rich painting.

Since LNG piping is in a cryogenic condition during use and is isolated from the external

environment with cold insulation, there is usually no SCC problem. However, should Invar alloy LNG piping be exposed to moisture during construction or during periodical stoppage, there is a possibility of SCC generation. Therefore, the SCC prevention measures to be employed should be selected based on the conditions to which the LNG piping is subjected during installation and operation.

## 5 Validation with Actual Piping System

A small-scale (12"x 20 m) Invar alloy test piping system (liquid nitrogen piping) was constructed (Fig. 12). The level of stress was measured at various parts of this piping system during a process of low-temperature cooling/pressurizing and a process of repeated cooling and heating. Through these tests, it was verified that there was no progressive increase of strain and that the robustness of the weld was maintained.

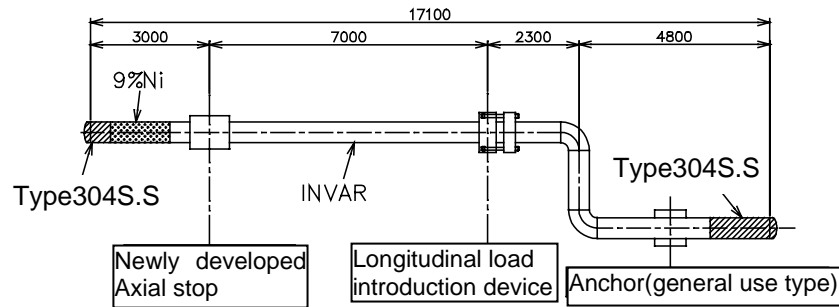


Fig. 12 Constitution of Invar alloy test piping

## 6. Construction of actual on-site INVAR ALLOY LNG piping

Prior to construction, variation of welding performance of several welders was researched, and then the welders were trained enough.

In the spring of 2001, an Invar alloy LNG piping was installed in the Osaka Gas Senboku Terminal II for the first time in the world (Photo 5).

This Invar alloy piping, which is 6" in diameter and 9.5mm thick, has been serving as an interconnection piping to an LNG vaporizer satisfactorily.

Moreover, this piping was inspected after 6-month service to verify its integrity.



Photo 5 Invar alloy LNG piping that serves as an interconnection piping to an LNG vaporizer

Now the second application of Invar alloy LNG piping as an interconnection piping to an LNG storage tank (180000kL,in LNG terminal at Himeji) is under construction and planned to be commissioned in August 2003. With evolved technologies, Invar alloy LNG piping of 28" and 10" in diameter has been realized.

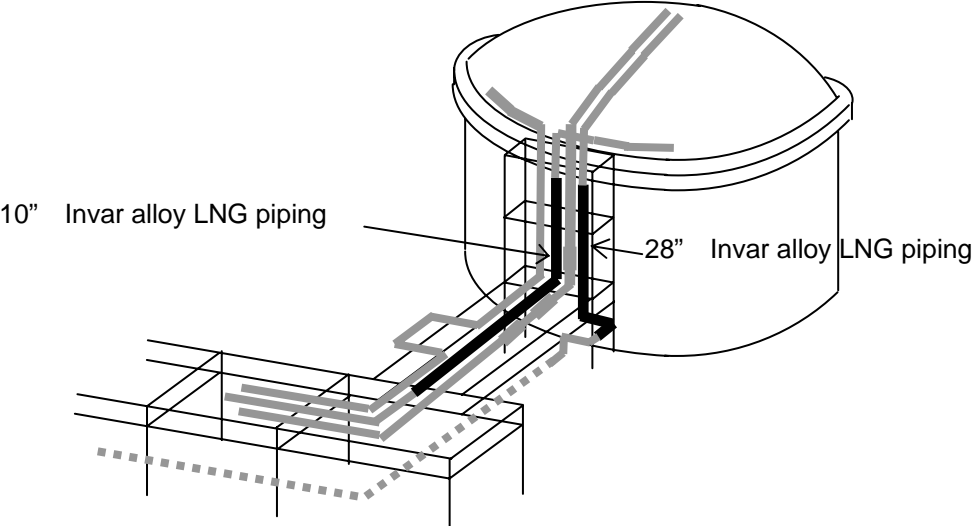


Fig. 13 Invar alloy LNG piping that serves as an interconnection piping to an LNG storage Tank

**7. CONCLUSION**

Through our research and development, application of Invar alloy to LNG piping has been established leading to reduction of construction cost. Next step of our plan is to extend more actual on-site applications of Invar alloy to the LNG piping.

It is expected that Invar alloy LNG piping would become widely used for LNG terminals contributing to cost reduction of gas industry.